Fractal-based RANS Modeling of Darrieus–Landau and Thermal-diffusive Instability Effects on Lean Hydrogen Flames

D. Zivkovic and T. Sattelmayer
Chair of Thermodynamics, Technical University of Munich (TUM)
Garching, Germany

1 Introduction

Accelerating flames, typical for large-scale explosions, are in absence of turbulence dominantly driven by the Darrieus-Landau (DL) instability [1]. As the flame grows, wrinkled under the influence of the DL instability, its characteristic self-similar structure can be observed [2–4]. The onset of cellular instabilities occurs for both lean and rich mixtures alike, once the flame reaches a critical distance [3], which itself is a function of stoichiometry [4]. Modeling the effects of DL instability is important for understanding and mitigation of industrial explosions, especially their early stages. Present work proposes an approach that is applicable to explosion simulation at large geometric scales. This is accomplished by a sub-grid closure, i.e. without resolving the flame structure.

2 Numerical Modeling

A numerical method [5] is used that solves unsteady, compressible, reacting flow equations by means of a density-based, all-speed, finite volume solver. The implementation is based on a widely known open-source code OpenFOAM. The reacting flow modeling is accomplished by solving a transport equation for the reaction progress variable b, defined as $b = 1$ in the unburned and $b = 0$ in the burned mixture [6]. The source term of the equation, representing the burning rate, is given as

$$\dot{\omega} = \rho_u \Xi S_l |\boldsymbol{\nabla} b| \tag{1}$$

where ρ_u is the unburnt mixture density, S_l the laminar flame speed, Ξ the flame wrinkling factor. Experimentally derived values for unstreched laminar flame speeds are used [7], corrected for the thermodynamic state according to [8]. The flame wrinkling factor Ξ represents a ratio between wrinkled and unwrinkled flame surfaces—its calculation is the main aim of the combustion model presented next.

The fractal theory [9] provides a general way of describing the wrinkled flame surface, according to which the flame wrinkling factor is

$$\Xi_{DL} = \left(\frac{\epsilon_o}{\epsilon_i} \right)^{\beta} \tag{2}$$

Correspondence to: zivkovic@td.mw.tum.de

where ϵ_i and ϵ_o are the inner and the outer cut-off scale and the exponent β is named fractal excess.

A novel modeling approach is developed in present work where the outer cut-off scale ϵ_o is given by a closure model. In that way, the model can be applied to cases where the outer cut-off scale is largely unresolved (sub-grid). The model assumes ϵ_o to be proportional to the flame von Karman length scale such that

$$\epsilon_o = C_{DL} L_{vk,f}. \tag{3}$$

Here, C_{DL} is the proportionality constant and the flame von Karman scale $L_{vk,f}$ is defined as

$$L_{vk,f} = \kappa_{vk} \left| \frac{\nabla \mathbf{U_f}}{\nabla^2 \mathbf{U_f}} \right| \tag{4}$$

where $\kappa_{vk} = 0.41$ is the von Karman constant, and $\mathbf{U_f}$ is the gas velocity field in the flame normal direction, defined as $\mathbf{U_f} = \mathbf{n_f} (\mathbf{n_f} \cdot \mathbf{U})$, where $n_f = \frac{\nabla b}{|\nabla b|}$ is the unit normal vector of the flame surface. The definition of the outer cut-off scale is based on an observation that, for the flames wrinkled by the DL instability, the hydrodynamic strain caused by thermal expansion is directly evidenced by the velocity gradient field. An assumption that the scale of flame wrinkling is proportional to the scale of hydrodynamic perturbations is in line with the understanding of the DL-wrinkled flame as a vortex sheet [1]. A similarly defined von Karman scale, albeit without the relation to the flame front normal, was used for estimating the length scale of resolved turbulent flow structures by scale-adaptive URANS turbulence models in [10].

In conditions of negligible turbulence, the inner cut-off scale can be assumed to be equal to the laminar flame thickness

$$\epsilon_i = \delta_l = \frac{\lambda_u}{\rho_u c_{p,u} S_l}. \tag{5}$$

With that, Eq. 2 becomes,

$$\Xi_{DL} = \left(\frac{C_{DL} L_{vk,f}}{\delta_l} \right)^{\beta} \tag{6}$$

where the proportionality constant was found to be $C_{DL} = 0.5$. An experimentally derived fractal excess β can be used, which was found by [4] to be $\beta = 0.243$ for hydrogen-air mixtures.

When lean hydrogen flames are considered, there are additional factors influencing the flame speed in addition to wrinkling induced by Darrieus-Landau instability. The influence of the thermal-diffusive (TD) instability on the flame wrinkling is modeled by the effective Lewis number approach

$$\Xi_{TD} = Le_{eff}^{-0.8} \tag{7}$$

as described in [8]. Furthermore, the influence of local curvature on the flame speed is taken into account by

$$F_c = (1 + \mathcal{L}\kappa)^{-1}. \tag{8}$$

Here, κ is the geometric small-scale local curvature defined in [8] to be $\kappa = \frac{\pi}{2} \kappa_{ref} \left(p/p_{ref}\right)^{0.55}$ using OH-PLIF experiments and highly resolved two-dimensional simulations of propagating flames, where κ_{ref} = 500 m^{-1} and p_{ref} = 1 bar. Furthermore, $\mathcal{L}$ is the Markstein length, derived empirically from the data of multiple experimental investigations [11–14].

The final flame wrinkling factor, including above-described individual contributions is given by

$$\Xi = \Xi_{DL} \cdot \Xi_{TD} \cdot F_c. \tag{9}$$

3 Model Validation and Discussion

3.1 Spherical Flame Propagation [4]

Model validation is first shown on a geometrically simple case of a spherically propagating flame in conditions of negligible initial turbulence. The validation data comes from experiments [4] performed in a rectangular 64 m^3 vented enclosure with homogeneous lean hydrogen mixtures. Flame position data was measured in the area that is 0.6 m in diameter. The computational setup for this case consists of a large enough domain to ensure boundary conditions do not interfere with the flame propagation initiated in the middle. The domain was discretized by an unstructured polyhedral computational grid with uniformly distributed cell size of approx. $\sqrt[3]{V_{cell}} = 90\,mm$. The advantage of polyhedral meshes is their efficiency when applied with FVM, and general ease of automatic generation. Flame propagation was initiated by switching the progress variable to burnt state in the middle of the domain. After ignition, the flame propagated outwards in all directions. Gravity was neglected in the computational setup since a spherical shape of the flame was observed in the experiments [4], leading to the conclusion that gravity effects did not play a significant influence.

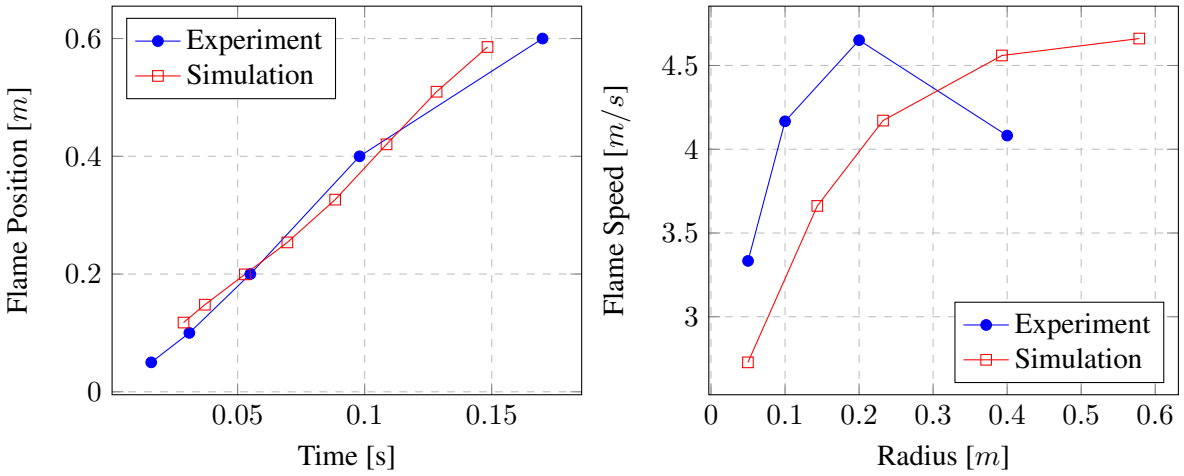

Figure 1: Spherical flame propagation [4] results for the $x_{H_2} = 12\%$ mixture. Left: change in the position of the flame in time. Right: change in observable flame speed along the flame radius.

Two lean hydrogen-air mixtures are shown in the results: first with $x_{H_2} = 12\%$ vol. (Fig.1) and second with $x_{H_2} = 19.08\%$ vol. (Fig.2). Left sides of both figures show the time evolution of the flame position and the right side shows the change in the observable flame speed along the flame trajectory (i.e. radius). The flame position was defined by the value of reaction progress variable $b = 0.5$. The model reproduces the flame's accelerating (exponential) behavior. The observable flame speed is slightly underpredicted in the simulations, despite of which the results of the flame position agree well with the experiments for both hydrogen contents.

A steep drop in flame speed is visible between the fourth and fifth measurement location (r $> 0.4\ m$) in the experimental results. Generally, the flame acceleration in a homogeneous mixture is expected to follow the exponential acceleration curve [2, 3]. Although this slowdown was not discussed in [4], it is possible that it originates from dilution of the fuel mixture by the surrounding air, happening at distances further away form the center of the test rig—an effect that was reported in a similar, large-scale hydrogen deflagration experiment in [15]. In the simulations, flame speeds seem to be approaching an asymptotic value that is mixture dependent.

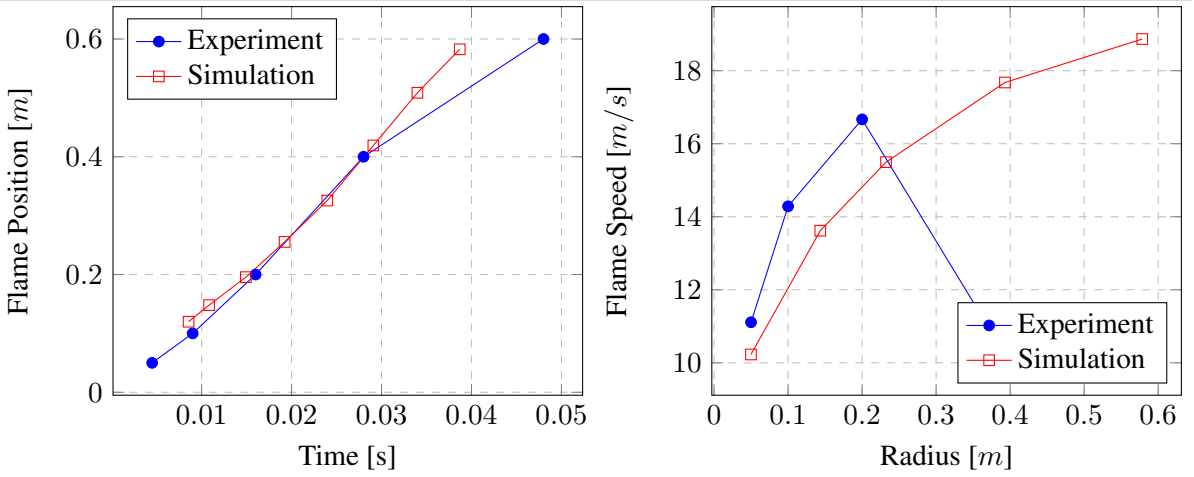

Figure 2: Spherical flame propagation [4] results for the $x_{H_2} = 19.08\%$ mixture. Left: change in the position of the flame in time. Right: change in observable flame speed along the flame radius.

3.2 Hydrogen Deflagration in the THAI Facility [16]

The second validation case is concerned with large-scale hydrogen deflagration in the THAI [16] test vessel. Experiments were conducted in a cylindrical vessel, 9.2 m in height and 3.2 m in diameter with a total volume of 60 m^3. A simulation was carried out for the test HD12 [16], where a homogeneous $x_{H_2} = 8\%$ vol. mixture was ignited near the bottom of the vessel. The computational domain considers the entire vessel volume, discretized into an unstructured polyhedral grid of uniformly-sized (approx. $\sqrt[3]{V_{cell}} = 200\ mm$) control volumes. Considering the significant height of the vessel, gravitational effects were taken into account. The ignition was accomplished by changing the value of the progress variable in a single control volume at the experimental ignition location. During ignition, the increase in the burnt fraction was calculated from the time necessary for the flame to travel the entirety of the control volume at the laminar flame speed.

Fig. 3 shows the time evolution of the flame vertical position along the vessel centerline (Fig. 3, left) and the observable flame speed along the vessel centerline (Fig. 3, right). Both show a good agreement between experiments and simulations. The pressure plot in the Fig. 4 shows simulations predicting a higher pressure peak, together with an earlier rise in pressure. The possible explanation could be that only sensible heat transfer to the vessel wall was considered in present work, while no radiation modeling was applied. It was concluded in the benchmarking exercise in [16] that computational models which included appropriate heat transfer modeling obtained better agreement with the pressure measurements in both predicting the pressure peak, as well as its time-evolution. The the difference in peak pressure between models with, and without heat losses modeling could be as high as 0.75 bar [16]. Although the THAI facility had no means of quantifying the relative importance of different heat transfer mechanisms [16], computational work by [17] suggests that radiative heat transfer played the most significant role in overall heat loss. Considering that, addition of a radiation model is planned for future work.

Pressure oscillations near the peak that are present in the simulations, have not been measured for the experimental case HD12, although oscillations due to parametric instability did occur in cases with different hydrogen content, e.g. HD22 [16]. It remains to be investigated whether these oscillations persist after radiation heat transfer is modeled, which can be expected to reduce the overall pressure level.

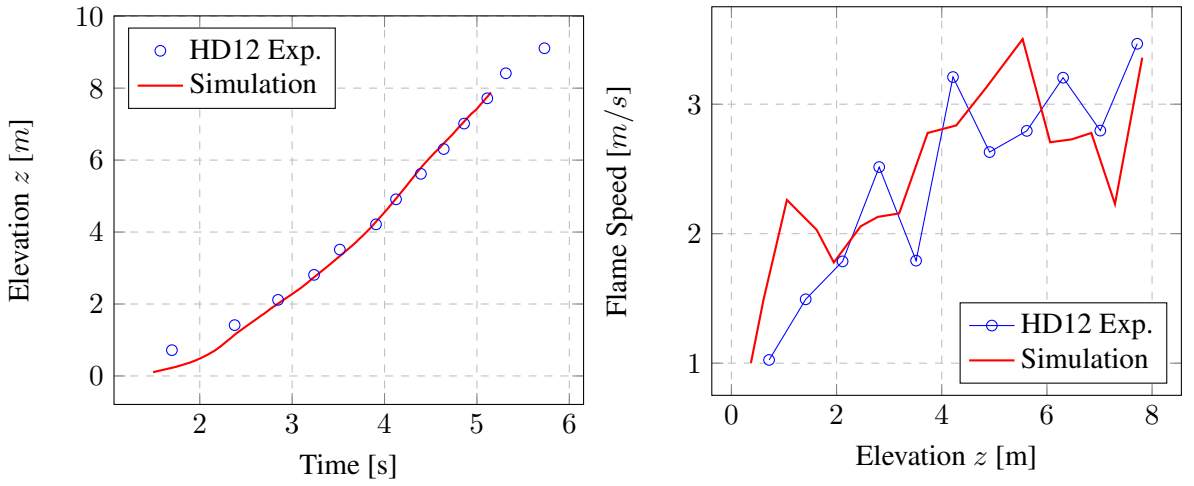

Figure 3: Hydrogen deflagration case HD12 ($x_{H_2} = 8\%$), THAI vessel [16]. Left: change in the flame vertical position in time. Right: change in observable flame speed along the vessel center line.

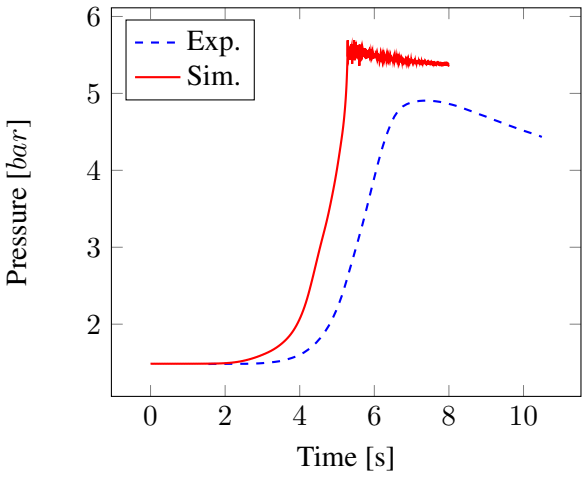

Figure 4: Pressure rise in time for the THAI [16] hydrogen deflagration case HD12 ($x_{H_2} = 8\%$).

4 Conclusions and Future Work

The present work introduced a new sub-grid modeling concept for Darrieus–Landau instability effects on lean hydrogen flames. The model is suitable for RANS simulations and uses scale-adaptive, fractal-based closure. The advantage of the model is that it allows for industrial-scale explosion simulation without prohibitive computational cost.

Model validation was performed on medium and large scale experiments, using coarse grids (where the grid spacing is significantly larger than the laminar flame thickness $\Delta x \gg \delta_l$), in conditions of negligible turbulence and in presence of gravitational effects.

There are several considerations, important for the application in the explosion safety domain—especially related to nuclear reactor accidents—that the developed model remains to be validated for. Those include the presence of diluents such as inert steam, and the presence of additional fuels such as carbon-monoxide. Finally, considering the significance of heat losses due to thermal radiation in slow deflagration cases, an appropriate radiation model would improve the overall modeling approach.

References

[1] Matalon, M. (2018). The Darrieus–Landau instability of premixed flames. Fl. Dyn. Res., 50(5).

[2] Bradley, D, Cresswell, TM, Puttock, JS (2001). Flame acceleration due to flame-induced instabilities in large-scale explosions. Combustion and Flame, 124(4), 551-559.

[3] Kim, WK, Mogi, T, Dobashi, R (2013). Flame acceleration in unconfined hydrogen/air deflagrations using infrared photography. Jour. of Loss Preven. in the Proc. Ind., 26(6), 1501-1505.

[4] Bauwens, CRL, Bergthorson, JM, Dorofeev, SB (2017). Experimental investigation of spherical-flame acceleration in lean hydrogen-air mixtures. Int. Jour. of Hid. Ener., 42(11), 7691-7697.

[5] Zivkovic, D, Sattelmayer, T (2021). Towards efficient and time-accurate simulations of early stages of industrial scale explosions (Accepted). 9th Int. Conf. on Hydrogen Safety (ICHS 2021).

[6] Weller, HG, Tabor, G, Gosman, AD, Fureby, C (1998). Application of a flame-wrinkling LES combustion model to a turbulent mixing layer. Int. Sym. on Comb. 27(1), 899-907.

[7] Konnov, AA (2008). Remaining uncertainties in the kinetic mechanism of hydrogen combustion. Combustion and Flame, 152(4), 507-528.

[8] Katzy, P (2020). Combustion model for the computation of flame propagation in lean hydrogen-air mixtures at low turbulence, Doctoral Diss., Technical University Munich.

[9] Gouldin, F. C. (1987). An application of fractals to modeling premixed turbulent flames. Combustion and flame, 68(3), 249-266.

[10] Menter, F. R., Egorov, Y. (2010). The scale-adaptive simulation method for unsteady turbulent flow predictions. Part 1: theory and model description. Flow, Turb. & Comb., 85(1), 113-138.

[11] Taylor, SC (1991). Burning velocity and the influence of flame stretch, Doct. Diss., Uni. of Leeds.

[12] Dowdy, DR, Smith, DB, Taylor, SC, Williams, A (1991). The use of expanding spherical flames to determine burning velocities and stretch effects in hydrogen/air mixtures. Int. Sym. on Comb. 23(1) 325-332.

[13] Lamoureux, N, Djebali-Chaumeix, N, Paillard, CE (2003). Lam. flame velocity determination for H2–air–He–CO2 mixtures using the spherical bomb method. Exp. Th. & Fl. Sci., 27(4), 385-393.

[14] Aung, KT, Hassan, MI, Faeth, GM (1997). Flame stretch interactions of laminar premixed hydrogen/air flames at normal temperature and pressure. Combustion and flame, 109(1-2), 1-24.

[15] Molkov, V, Makarov, D, Schneider, H (2006). LES modelling of an unconfined large-scale hydrogenair deflagration. J. Phys. D: Appl. Phys., 39(20), 4366.

[16] Kotchourko, A, Bentaib, A, Fischer, K, Chaumeix, N, Yanez, J, Benz, S, Kudryakov, S (2012). ISP-49 on hydrogen combustion. Nuc. Ener. Agency Committee on the Saf. of Nuc. Installations.

[17] Sathiah, P, Holler, T, Kljenak, I, Komen, E (2016). The role of CFD combustion modeling in hydrogen safety managementV: Validation for slow deflagrations in homogeneous hydrogen-air experiments. Nuc. Eng. Des., 310, 520-531.